Eur. Phys. J. C (2021) 81:52
https://doi.org/10.1140/epjc/s10052-021-08845-y

THE EUROPEAN PHYSICAL JOURNAL C

Regular Article - Theoretical Physics

Towards unification of quark and lepton flavors in A_4 modular invariance

Hiroshi Okada[1,2,a], **Morimitsu Tanimoto**[3,b]

[1] Asia Pacific Center for Theoretical Physics, Pohang 37673, Republic of Korea
[2] Department of Physics, Pohang University of Science and Technology, Pohang 37673, Republic of Korea
[3] Department of Physics, Niigata University, Niigata 950-2181, Japan

Received: 22 June 2020 / Accepted: 8 January 2021 / Published online: 19 January 2021

Abstract We study quark and lepton mass matrices in the A_4 modular symmetry towards the unification of the quark and lepton flavors. We adopt modular forms of weights 2 and 6 for quarks and charged leptons, while we use modular forms of weight 4 for the neutrino mass matrix which is generated by the Weinberg operator. We obtain the successful quark mass matrices, in which the down-type quark mass matrix is constructed by modular forms of weight 2, but the up-type quark mass matrix is constructed by modular forms of weight 6. The viable region of τ is close to $\tau = i$. Lepton mass matrices also work well at nearby $\tau = i$, which overlaps with the one of the quark sector, for the normal hierarchy of neutrino masses. In the common τ region for quarks and leptons, the predicted sum of neutrino masses is 87–120 meV taking account of its cosmological bound. Since both the Dirac CP phase δ^{ℓ}_{CP} and $\sin^2\theta_{23}$ are correlated with the sum of neutrino masses, improving its cosmological bound provides crucial tests for our scheme as well as the precise measurement of $\sin^2\theta_{23}$ and δ^{ℓ}_{CP}. The effective neutrino mass of the $0\nu\beta\beta$ decay is $\langle m_{ee}\rangle = 15$–$31$ meV. It is remarked that the modulus τ is fixed at nearby $\tau = i$ in the fundamental domain of SL(2, Z), which suggests the residual symmetry Z_2 in the quark and lepton mass matrices. The inverted hierarchy of neutrino masses is excluded by the cosmological bound of the sum of neutrino masses.

1 Introduction

The standard model (SM) was well established by the discovery of the Higgs boson. However, the flavor theory of quarks and leptons is still unknown. In order to understand the origin of the flavor structure, many works have appeared by using the discrete groups for flavors. In the early models of quark masses and mixing angles, the S_3 symmetry was used [1,2]. It was also discussed to understand the large mixing angle [3] in the oscillation of atmospheric neutrinos [4]. For the last twenty years, the discrete symmetries of flavors have been developed, that is motivated by the precise observation of flavor mixing angles of leptons [5–13].

Many models have been proposed by using the non-Abelian discrete groups S_3, A_4, S_4, A_5 and other groups with larger orders to explain the large neutrino mixing angles. Among them, the A_4 flavor model is an attractive one because the A_4 group is the minimal one including a triplet irreducible representation, which allows for a natural explanation of the existence of three families of leptons [14–20]. However, the variety of models is so wide that it is difficult to obtain a clear evidence of the A_4 flavor symmetry.

Recently, a new approach to the lepton flavor problem appeared based on the invariance under the modular group [21], where the model of the finite modular group $\Gamma_3 \simeq A_4$ has been presented. This work inspired further studies of the modular invariance approach to the lepton flavor problem. It should be emphasized that there is a significant difference between the models based on the A_4 modular symmetry and those based on the usual non-Abelian discrete A_4 flavor symmetry. Yukawa couplings transform non-trivially under the modular group and are written in terms of modular forms which are holomorphic functions of the modulus τ.

The modular group includes the finite groups S_3, A_4, S_4, and A_5 [22]. Therefore, an interesting framework for the construction of flavor models has been put forward based on the $\Gamma_3 \simeq A_4$ modular group [21], and further, based on $\Gamma_2 \simeq S_3$ [23]. The proposed flavor models with modular symmetries $\Gamma_4 \simeq S_4$ [24] and $\Gamma_5 \simeq A_5$ [25] have also stimulated studies of flavor structures of quarks and leptons. Phenomenological discussions of the neutrino flavor mixing have been done based on A_4 [26,27], S_4 [28,29], A_5 [30], and T' [31]

[a] e-mail: hiroshi.okada@apctp.org (corresponding author)
[b] e-mail: tanimoto@muse.sc.niigata-u.ac.jp

modular groups, respectively. In particular, the comprehensive analysis of the A_4 modular group has provided a distinct prediction of the neutrino mixing angles and the CP violating phase [27]. The A_4 modular symmetry has been also applied to the $SU(5)$ grand unified theory (GUT) of quarks and leptons [32], while the residual symmetry of the A_4 modular symmetry has been investigated phenomenologically [33]. Furthermore, modular forms for $\Delta(96)$ and $\Delta(384)$ were constructed [34], and the extension of the traditional flavor group is discussed with modular symmetries [35]. Moreover, multiple modular symmetries are proposed as the origin of flavor [36]. The modular invariance has been also studied combining with the generalized CP symmetries for theories of flavors [37]. The quark mass matrix has been discussed in the S_3 and A_4 modular symmetries as well [38–40].

Besides mass matrices of quarks and leptons, related topics have been discussed in the baryon number violation [38], the dark matter [41,42] and the modular symmetry anomaly [43].

In this work, we study both quark and lepton mass matrices in the A_4 modular symmetry. If flavors of quarks and leptons are originated from a same two-dimensional compact space, quarks and leptons have the same flavor symmetry and the same value of the modulus τ. Therefore, it is challenging to reproduce observed three Cabibbo–Kobayashi–Maskawa (CKM) mixing angles and the CP violating phase while observed large mixing angles in the lepton sector within the framework of the A_4 modular invariance with the common τ. This work provides a new aspect in order to discover the unification theory of the quark and lepton flavors. We have already discussed the quark mass matrices in terms of A_4 modular forms of weight 2 [40]. It has been found that quark mass matrices of A_4 do not work unless Higgs sector is extended by A_4 triplet representations. In this paper, we propose to adopt modular forms of weight 6 in addition to modular ones of weight 2 for quarks with the Higgs sector of SM. We use modular forms of weight 4 for the neutrino mass matrix, which is generated by the Weinberg operator. The common value of the modulus τ is successfully obtained by using observed four CKM matrix elements and three lepton mixing angles. We also predict the CP violating Dirac phase of leptons, which is expected to be observed at T2K and NOνA experiments [44,45], and the sum of neutrino masses.[1]

The paper is organized as follows. In Sect. 2, we give a brief review on the modular symmetry and modular forms of weights 2, 4 and 6. In Sect. 3, we present the model for quark mass matrices in the A_4 modular symmetry. In Sect. 4, we show numerical results for the CKM matrix. In Sect. 5, we discuss the lepton mass matrices and present numerical results. Section 6 is devoted to a summary. In Appendix A, the tensor product of the A_4 group is presented. In Appendix B, we present how to obtain Dirac CP phase, Majorana phases and effective mass of the $0\nu\beta\beta$ decay.

[1] In order to reduce the number of parameters, we discussed another A_4 quark/lepton mass matrices after this work [46]. However, the sum of neutrino masses is predicted to be larger than the cosmological upper-bound, 120 meV. Indeed, a model with two parameters fewer than the present model gives 140 meV for the sum of neutrino masses.

2 Modular group and modular forms of weights 2, 4, 6

The modular group $\bar{\Gamma}$ is the group of linear fractional transformations γ acting on the modulus τ, belonging to the upper-half complex plane as:

$$\tau \longrightarrow \gamma\tau = \frac{a\tau + b}{c\tau + d}, \quad \text{where} \quad a, b, c, d \in \mathbb{Z} \quad \text{and} \quad ad - bc = 1, \quad \text{Im}[\tau] > 0, \tag{1}$$

which is isomorphic to $PSL(2,\mathbb{Z}) = SL(2,\mathbb{Z})/\{I, -I\}$ transformation. This modular transformation is generated by S and T,

$$S : \tau \longrightarrow -\frac{1}{\tau}, \quad T : \tau \longrightarrow \tau + 1, \tag{2}$$

which satisfy the following algebraic relations,

$$S^2 = \mathbb{I}, \quad (ST)^3 = \mathbb{I}. \tag{3}$$

We introduce the series of groups $\Gamma(N)$ ($N = 1, 2, 3, \dots$), called principal congruence subgroups, defined by

$$\Gamma(N) = \left\{ \begin{pmatrix} a & b \\ c & d \end{pmatrix} \in SL(2,\mathbb{Z}), \quad \begin{pmatrix} a & b \\ c & d \end{pmatrix} = \begin{pmatrix} 1 & 0 \\ 0 & 1 \end{pmatrix} \pmod{N} \right\}. \tag{4}$$

For $N = 2$, we define $\bar{\Gamma}(2) \equiv \Gamma(2)/\{I, -I\}$. Since the element $-I$ does not belong to $\Gamma(N)$ for $N > 2$, we have $\bar{\Gamma}(N) = \Gamma(N)$. The quotient groups defined as $\Gamma_N \equiv \bar{\Gamma}/\bar{\Gamma}(N)$ are finite modular groups. In this finite groups Γ_N, $T^N = \mathbb{I}$ is imposed. The groups Γ_N with $N = 2, 3, 4, 5$ are isomorphic to S_3, A_4, S_4 and A_5, respectively [22].

Modular forms of level N are holomorphic functions $f(\tau)$ transforming under $\Gamma(N)$ as:

$$f(\gamma\tau) = (c\tau + d)^k f(\tau), \quad \gamma \in \Gamma(N), \tag{5}$$

where k is the so-called as the modular weight.

Superstring theory on the torus T^2 or orbifold T^2/Z_N has the modular symmetry [47–53]. Its low energy effective field theory is described in terms of supergravity theory, and string-derived supergravity theory has also the modular symmetry. Under the modular transformation of Eq. (1), chiral superfields $\phi^{(I)}$ transform as [54],

$$\phi^{(I)} \to (c\tau + d)^{-k_I} \rho^{(I)}(\gamma)\phi^{(I)}, \tag{6}$$

where $-k_I$ is the modular weight and $\rho^{(I)}(\gamma)$ denotes a unitary representation matrix of $\gamma \in \bar{\Gamma}$.

In the present article we study global supersymmetric models, e.g., minimal supersymmetric extensions of the Standard Model (MSSM). The superpotential which is built from matter fields and modular forms is assumed to be modular invariant, i.e., to have a vanishing modular weight. For given modular forms this can be achieved by assigning appropriate weights to the matter superfields.

The kinetic terms are derived from a Kähler potential. The Kähler potential of chiral matter fields $\phi^{(I)}$ with the modular weight $-k_I$ is given simply by

$$K^{\text{matter}} = \frac{1}{[i(\bar{\tau}-\tau)]^{k_I}} |\phi^{(I)}|^2, \tag{7}$$

where the superfield and its scalar component are denoted by the same letter, and $\bar{\tau} = \tau^*$ after taking the vacuum expectation value (VEV).[2] Therefore, the canonical form of the kinetic terms is obtained by changing the normalization of parameters [27].

For $\Gamma_3 \simeq A_4$, the dimension of the linear space $\mathcal{M}_k(\Gamma(3))$ of modular forms of weight k is $k+1$ [56–58], i.e., there are three linearly independent modular forms of the lowest nontrivial weight 2. These forms have been explicitly obtained [21] in terms of the Dedekind eta-function $\eta(\tau)$:

$$\eta(\tau) = q^{1/24}\prod_{n=1}^{\infty}(1-q^n), \quad q = \exp\,(i2\pi\tau), \tag{8}$$

where $\eta(\tau)$ is a so called modular form of weight $1/2$. In what follows we will use the following basis of the A_4 generators S and T in the triplet representation:

$$S = \frac{1}{3}\begin{pmatrix} -1 & 2 & 2 \\ 2 & -1 & 2 \\ 2 & 2 & -1 \end{pmatrix}, \quad T = \begin{pmatrix} 1 & 0 & 0 \\ 0 & \omega & 0 \\ 0 & 0 & \omega^2 \end{pmatrix}, \tag{9}$$

where $\omega = \exp(i\frac{2}{3}\pi)$. The modular forms of weight 2 transforming as a triplet of A_4 can be written in terms of $\eta(\tau)$ and its derivative [21]:

$$\begin{aligned} Y_1(\tau) &= \frac{i}{2\pi}\left(\frac{\eta'(\tau/3)}{\eta(\tau/3)} + \frac{\eta'((\tau+1)/3)}{\eta((\tau+1)/3)} + \frac{\eta'((\tau+2)/3)}{\eta((\tau+2)/3)} \right. \\ &\quad \left. - \frac{27\eta'(3\tau)}{\eta(3\tau)}\right), \\ Y_2(\tau) &= \frac{-i}{\pi}\left(\frac{\eta'(\tau/3)}{\eta(\tau/3)} + \omega^2\frac{\eta'((\tau+1)/3)}{\eta((\tau+1)/3)} + \omega\frac{\eta'((\tau+2)/3)}{\eta((\tau+2)/3)}\right), \\ Y_3(\tau) &= \frac{-i}{\pi}\left(\frac{\eta'(\tau/3)}{\eta(\tau/3)} + \omega\frac{\eta'((\tau+1)/3)}{\eta((\tau+1)/3)} + \omega^2\frac{\eta'((\tau+2)/3)}{\eta((\tau+2)/3)}\right). \end{aligned} \tag{10}$$

[2] The most general Kähler potential consistent with the modular symmetry possibly contains additional terms, as recently pointed out in Ref. [55]. However, we consider only the simplest form of the Kähler potential.

The overall coefficient in Eq. (10) is one possible choice. It cannot be uniquely determined. The triplet modular forms of weight 2 have the following q-expansions:

$$\mathbf{Y_3^{(2)}} = \begin{pmatrix} Y_1(\tau) \\ Y_2(\tau) \\ Y_3(\tau) \end{pmatrix} = \begin{pmatrix} 1 + 12q + 36q^2 + 12q^3 + \cdots \\ -6q^{1/3}(1 + 7q + 8q^2 + \cdots) \\ -18q^{2/3}(1 + 2q + 5q^2 + \cdots) \end{pmatrix}. \tag{11}$$

They satisfy also the constraint [21]:

$$(Y_2(\tau))^2 + 2Y_1(\tau)Y_3(\tau) = 0. \tag{12}$$

The modular forms of the higher weight, k, can be obtained by the A_4 tensor products of the modular forms with weight 2, $\mathbf{Y_3^{(2)}}$, as given in Appendix A. For weight 4, that is $k = 4$, there are five modular forms by the tensor product of $\mathbf{3} \otimes \mathbf{3}$ as:

$$\begin{aligned} &\mathbf{Y_1^{(4)}} = Y_1^2 + 2Y_2Y_3, \quad \mathbf{Y_{1'}^{(4)}} = Y_3^2 + 2Y_1Y_2, \\ &\mathbf{Y_{1''}^{(4)}} = Y_2^2 + 2Y_1Y_3 = 0, \\ &\mathbf{Y_3^{(4)}} = \begin{pmatrix} Y_1^{(4)} \\ Y_2^{(4)} \\ Y_3^{(4)} \end{pmatrix} = \begin{pmatrix} Y_1^2 - Y_2Y_3 \\ Y_3^2 - Y_1Y_2 \\ Y_2^2 - Y_1Y_3 \end{pmatrix}, \end{aligned} \tag{13}$$

where $\mathbf{Y_{1''}^{(4)}}$ vanishes due to the constraint of Eq. (12). For weight 6, there are seven modular forms by the tensor products of A_4 as:

$$\mathbf{Y_1^{(6)}} = Y_1^3 + Y_2^3 + Y_3^3 - 3Y_1Y_2Y_3\,,$$

$$\begin{aligned} \mathbf{Y_3^{(6)}} &\equiv \begin{pmatrix} Y_1^{(6)} \\ Y_2^{(6)} \\ Y_3^{(6)} \end{pmatrix} = \begin{pmatrix} Y_1^3 + 2Y_1Y_2Y_3 \\ Y_1^2Y_2 + 2Y_2^2Y_3 \\ Y_1^2Y_3 + 2Y_3^2Y_2 \end{pmatrix}, \\ \mathbf{Y_{3'}^{(6)}} &\equiv \begin{pmatrix} Y_1^{'(6)} \\ Y_2^{'(6)} \\ Y_3^{'(6)} \end{pmatrix} = \begin{pmatrix} Y_3^3 + 2Y_1Y_2Y_3 \\ Y_3^2Y_1 + 2Y_1^2Y_2 \\ Y_3^2Y_2 + 2Y_2^2Y_1 \end{pmatrix}. \end{aligned} \tag{14}$$

By using these modular forms of weights 2, 4 and 6, we discuss quark and lepton mass matrices.

3 Quark mass matrices in the A_4 modular invariance

Let us consider a A_4 modular invariant flavor model for quarks. There are freedoms for the assignments of irreducible representations and modular weights to quarks and Higgs doublets.

The simplest one is to assign the triplet of the A_4 group to three left-handed quarks, but three different singlets

Table 1 Assignments of representations and weights $-k_I$ for MSSM fields and modular forms

	Q	$(d^c,\ s^c,\ b^c)$	$(u^c,\ c^c,\ t^c)$	H_q	$\mathbf{Y_3^{(2)}},\ \mathbf{Y_3^{(6)}},\ \mathbf{Y_{3'}^{(6)}}$
$SU(2)$	**2**	**1**	**1**	**2**	**1**
A_4	**3**	$(\mathbf{1}, \mathbf{1}'', \mathbf{1}')$	$(\mathbf{1}, \mathbf{1}'', \mathbf{1}')$	**1**	**3**, **3**, **3′**
$-k_I$	-2	$(0,\ 0,\ 0)$	$(-4,\ -4,\ -4)$	0	$k=2$, $k=6$, $k=6$

$(\mathbf{1}, \mathbf{1}'', \mathbf{1}')$ of A_4 to the three right-handed quarks, (u^c, c^c, t^c) and (d^c, s^c, b^c), respectively, where the sum of weights of the left-handed and the right-handed quarks is -2. The Higgs fields are supposed to be A_4 singlets with weight 0. Then, three independent couplings appear in the superpotential of the up-type and down-type quark sectors, respectively, as follows:

$$w_u = \alpha_u u^c H_u \mathbf{Y_3^{(2)}} Q + \beta_u c^c H_u \mathbf{Y_3^{(2)}} Q + \gamma_u t^c H_u \mathbf{Y_3^{(2)}} Q, \tag{15}$$

$$w_d = \alpha_d d^c H_d \mathbf{Y_3^{(2)}} Q + \beta_d s^c H_d \mathbf{Y_3^{(2)}} Q + \gamma_d b^c H_d \mathbf{Y_3^{(2)}} Q, \tag{16}$$

where Q is the left-handed A_4 triplet quarks, and H_q is the Higgs doublet. The parameters α_q, β_q, γ_q are constant coefficients. Assign the A_4 triplet Q as $((d_L, u_L), (s_L, c_L), (b_L, t_L))$. By using the decomposition of the A_4 tensor product in Appendix A, the superpotentials in Eqs. (15) and (16) give the mass matrix of quarks, which is written in terms of modular forms of weight 2 as:

$$M_q = v_q \begin{pmatrix} \alpha_q & 0 & 0 \\ 0 & \beta_q & 0 \\ 0 & 0 & \gamma_q \end{pmatrix} \begin{pmatrix} Y_1 & Y_3 & Y_2 \\ Y_2 & Y_1 & Y_3 \\ Y_3 & Y_2 & Y_1 \end{pmatrix}_{RL}, \quad (q = u, d), \tag{17}$$

where τ of the modular forms $Y_i(\tau)$ is omitted. The constant v_q $(q = u, d)$ is the VEV of the neutral component of the Higgs field H_q. Parameters α_q, β_q, γ_q are taken to be real without loss of generality, and they can be adjusted to the observed quark masses. The remained parameter is only the modulus τ. The numerical study of the quark mass matrix in Eq. (17) is rather easy. However, it is impossible to reproduce observed hierarchical three CKM mixing angles by fixing one complex parameter τ.

In order to obtain realistic quark mass matrices, we use modular forms of weight 6 in Eq. (14). As a simple model, we take modular forms of weight 6 only for the up-type quark mass matrix while the down-type quark one is still given in terms of modular forms of weight 2 such as Eq. (17).[3]

[3] We also take modular forms of weight 2 for the charged lepton mass matrix to give a minimal number of parameters in the lepton sector.

Then, we have six independent couplings in the superpotential of the up-quark sector as:

$$\begin{aligned} w_u = {} & \alpha_u u^c H_u \mathbf{Y_3^{(6)}} Q + \alpha'_u u^c H_u \mathbf{Y_{3'}^{(6)}} Q + \beta_u c^c H_u \mathbf{Y_3^{(6)}} Q \\ & + \beta'_u c^c H_u \mathbf{Y_{3'}^{(6)}} Q + \gamma_u t^c H_u \mathbf{Y_3^{(6)}} Q \\ & + \gamma'_u t^c H_q \mathbf{Y_{3'}^{(6)}} Q, \end{aligned} \tag{18}$$

where assignments of representations and weights for MSSM fields are given in Table 1. The up-type quark mass matrix is written as:

$$\begin{aligned} M_u = v_u & \begin{pmatrix} \alpha_u & 0 & 0 \\ 0 & \beta_u & 0 \\ 0 & 0 & \gamma_u \end{pmatrix} \left[\begin{pmatrix} Y_1^{(6)} & Y_3^{(6)} & Y_2^{(6)} \\ Y_2^{(6)} & Y_1^{(6)} & Y_3^{(6)} \\ Y_3^{(6)} & Y_2^{(6)} & Y_1^{(6)} \end{pmatrix} \right. \\ & \left. + \begin{pmatrix} g_{u1} & 0 & 0 \\ 0 & g_{u2} & 0 \\ 0 & 0 & g_{u3} \end{pmatrix} \begin{pmatrix} Y_1^{'(6)} & Y_3^{'(6)} & Y_2^{'(6)} \\ Y_2^{'(6)} & Y_1^{'(6)} & Y_3^{'(6)} \\ Y_3^{'(6)} & Y_2^{'(6)} & Y_1^{'(6)} \end{pmatrix} \right]_{RL}, \end{aligned} \tag{19}$$

where $g_{u1} = \alpha'_u/\alpha_u$, $g_{u2} = \beta'_u/\beta_u$ and $g_{u3} = \gamma'_u/\gamma_u$ are complex parameters while α_u, β_u and γ_u are real.

On the other hand, the down-type quark mass matrix is given as:

$$M_d = v_d \begin{pmatrix} \alpha_d & 0 & 0 \\ 0 & \beta_d & 0 \\ 0 & 0 & \gamma_d \end{pmatrix} \begin{pmatrix} Y_1 & Y_3 & Y_2 \\ Y_2 & Y_1 & Y_3 \\ Y_3 & Y_2 & Y_1 \end{pmatrix}_{RL}. \tag{20}$$

We will fix the modulus τ phenomenologically by using quark mass matrices in Eqs. (19) and (20).

4 Fixing τ by observed CKM

In order to obtain the left-handed flavor mixing, we calculate $M_d^\dagger M_d$ and $M_u^\dagger M_u$. At first, we take a random point of τ and g_{ui} which are scanned in the complex plane by generating random numbers. The modulus τ is scanned in the fundamental domain of the modular symmetry. In practice, the scanned range of $\mathrm{Im}[\tau]$ is $[\sqrt{3}/2, 2]$, in which the lower-cut $\sqrt{3}/2$ is at the cusp of the fundamental domain, and the upper-cut 2 is enough large for estimating Y_i. On the other hand, $\mathrm{Re}[\tau]$ is scanned in the fundamental domain $[-1/2, 1/2]$ of the modular group. Supposing $|g_{ui}|$ is of order one, we scan them in $[0, 2]$ while these phases are scanned in $[-\pi, \pi]$. Then,

Table 2 Parameter ranges consistent with the observed CKM mixing angles and CP phase δ_{CP}

$\|\mathrm{Re}[\tau]\|$	$\mathrm{Im}[\tau]$	$\|g_{u1}\|$	Arg g_{u1}	$\|g_{u2}\|$	Arg g_{u2}	$\|g_{u3}\|$	Arg g_{u3}
[0, 0.09]	[0.99, 1.09]	[0.01, 0.86]	$[-\pi, \pi]$	[0.14, 1.29]	$[-2.3, 1.6]$	[0.02, 0.07]	$[-\pi, \pi]$

parameters $\alpha_q, \beta_q, \gamma_q$ $(q = u, d)$ are given in terms of τ and g_q after inputting six quark masses.

Finally, we calculate three CKM mixing angles and the CP violating phase in terms of the model parameters τ and g_{ui}. We keep the parameter sets, in which the value of each observable is reproduced within the three times of 1σ interval of error-bars. We continue this procedure to obtain enough points for plotting allowed region.

We input quark masses in order to constrain model parameters. Since the modulus τ obtains the expectation value by the breaking of the modular invariance at the high mass scale, the quark masses are put at the GUT scale. The observed masses and CKM parameters run to the GUT scale by the renormalization group equations (RGEs). In our work, we adopt numerical values of Yukawa couplings of quarks at the GUT scale 2×10^{16} GeV with $\tan\beta = 5$ in the framework of the minimal SUSY breaking scenarios [59,60]:

$$\begin{aligned} &y_d = (4.81 \pm 1.06) \times 10^{-6}, \quad y_s = (9.52 \pm 1.03) \times 10^{-5}, \\ &y_b = (6.95 \pm 0.175) \times 10^{-3}, \\ &y_u = (2.92 \pm 1.81) \times 10^{-6}, \quad y_c = (1.43 \pm 0.100) \times 10^{-3}, \\ &y_t = 0.534 \pm 0.0341, \end{aligned} \tag{21}$$

which give quark masses as $m_q = y_q v_H$ with $v_H = 174$ GeV.

We also use the following CKM mixing angles to focus on parameter regions consistent with the experimental data at the GUT scale 2×10^{16} GeV, where $\tan\beta = 5$ is taken [59,60]:

$$\begin{aligned} &\theta_{12}^{\mathrm{CKM}} = 13.027^\circ \pm 0.0814^\circ, \quad \theta_{23}^{\mathrm{CKM}} = 2.054^\circ \pm 0.384^\circ, \\ &\theta_{13}^{\mathrm{CKM}} = 0.1802^\circ \pm 0.0281^\circ. \end{aligned} \tag{22}$$

Here $\theta_{ij}^{\mathrm{CKM}}$ is given in the PDG notation of the CKM matrix V_{CKM} [61]. The CP violating phase is also given as:

$$\delta_{CP} = 69.21^\circ \pm 6.19^\circ, \tag{23}$$

in the PDG notation. The errors in Eqs. (21)–(23) represent 1σ interval. The CKM elements V_{ij} at the GUT scale 2×10^{16} GeV are given by using these angles and the phase.

In our model, we have four complex parameters, τ, g_{u1}, g_{u2} and g_{u3} after inputting six quark masses. These eight real parameters are scanned to reproduce the observed three

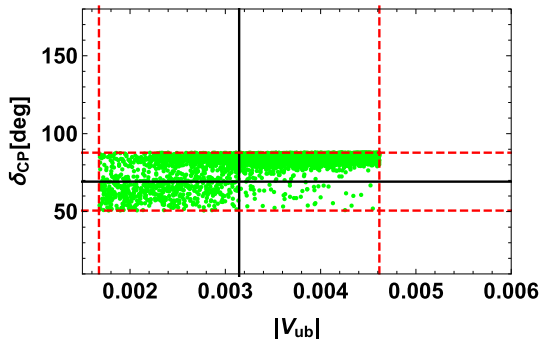

Fig. 1 Distribution on $|V_{ub}|$–δ_{CP} plane, where black lines denote observed central values of $|V_{ub}|$ and δ_{CP}, and red dashed-lines denote three times 1σ interval

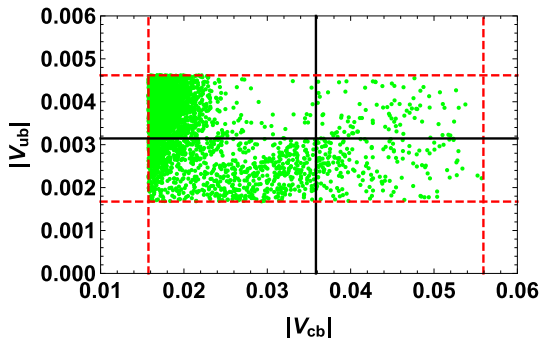

Fig. 2 Distribution on $|V_{cb}|$–$|V_{ub}|$ plane where black lines denote observed central values of $|V_{cb}|$ and $|V_{ub}|$, and red dashed-lines denote three times 1σ interval

CKM mixing angles and the CP violating phase with three times 1σ error interval in Eqs. (22) and (23).[4]

We have succeeded to reproduce completely four observed CKM elements in the parameter ranges of Table 2. The modulus τ is close to i, which is the fixed point of the modular symmetry.

In order to check the consistency of our quark mass matrices and the observed CKM, we show the calculated distribution on the $|V_{ub}|$–δ_{CP} plane at the GUT scale in Fig. 1. The calculated δ_{CP} is uniformly distributed below the observed central value of $|V_{ub}|$ while it is almost larger than the observed central value for the upper-range of $|V_{ub}|$.

We also present the distribution of CKM elements $|V_{cb}|$ and $|V_{ub}|$ at the GUT scale in Fig. 2. The magnitude of $|V_{ub}|$ is predicted to be in the whole region of the three times 1σ

[4] We take the observed values of CKM with three times 1σ intervals, which are almost 3σ in this case.

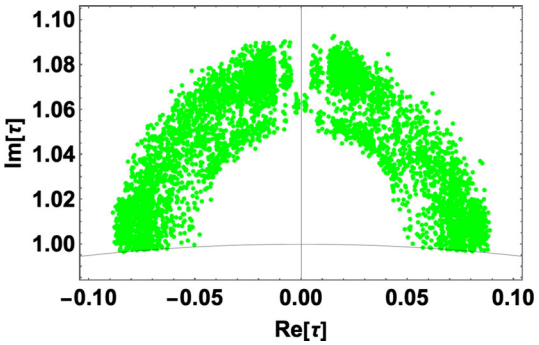

Fig. 3 The allowed region on Re[τ]–Im[τ] plane, where observed CKM mixing angles and δ_{CP} are reproduced. The solid curve is the boundary of the fundamental domain, $|\tau| = 1$

Table 3 Numerical values of parameters and output of CKM parameters at the best-fit point

τ	$-0.038 + 1.05\,i$
g_{u1}	$-0.147 + 0.118\,i$
g_{u2}	$-0.091 - 0.425\,i$
g_{u3}	$0.027 + 0.0197\,i$
α_u/γ_u	4.33×10^{-5}
β_u/γ_u	3.85×10^{-3}
α_d/γ_d	1.45×10^{-2}
β_d/γ_d	4.26×10^{-3}
$\lvert V_{us}\rvert$	0.225
$\lvert V_{cb}\rvert$	0.029
$\lvert V_{ub}\rvert$	0.0030
δ_{CP}	76.9°
χ^2	0.46

interval while the calculated $|V_{cb}|$ is mostly distributed in the lower-range of the three times 1σ interval.

In Fig. 3, we show the plot of Re[τ] and Im[τ], which will be compared with the case of leptons. The allowed region of the modulus τ is close to i, but is clearly deviated from it. The modulus $\tau = i$ is the fixed point of the modular symmetry. Indeed, $\tau = i$ is invariant under the S transformation $\tau = -1/\tau$, where the subgroup $\mathbb{Z}_2^S = \{\mathrm{I}, \mathrm{S}\}$ of A_4 is preserved. This region of τ is discussed in connection with τ of the lepton mass matrices in the next secton.

In Table 3, we present one parameter set and calculated CKM elements, which is the best-fit point, that is, its χ^2 is minimum. The magnitudes of g_{qi} are at most of order $\mathcal{O}(0.5)$. Ratios of α_q/γ_q and β_q/γ_q $(q = u, d)$ correspond to the observed quark mass hierarchy.

We also present the mixing matrices of up-type quarks and down-type quarks for the sample of Table 3. They are given as:

$$V_u \approx \begin{pmatrix} 0.987 & -0.017 + 0.142\,i & 0.056 - 0.039\,i \\ 0.029 + 0.148\,i & 0.960 & -0.236 - 0.014\,i \\ -0.048 - 0.004\,i & 0.241 - 0.021\,i & 0.969 \end{pmatrix},$$
$$V_d \approx \begin{pmatrix} 0.992 & 0.083 - 0.062\,i & 0.057 - 0.043\,i \\ -0.065 - 0.049\,i & 0.962 & -0.259 + 0.003\,i \\ -0.076 - 0.058\,i & 0.251 + 0.002\,i & 0.963 \end{pmatrix}, \quad (24)$$

where $V_{\mathrm{CKM}} = V_u^\dagger V_d$. It is noted that these are presented in the diagonal base of the generator S, where we can see the hierarchical structure of mixing. The diagonal base of S is realized by the unitary transformation of S in Eq. (9), $V_S\, S\, V_S^\dagger = \mathrm{diag}[1, -1, -1]$, where

$$V_S \equiv \begin{pmatrix} \frac{1}{\sqrt{3}} & \frac{1}{\sqrt{3}} & \frac{1}{\sqrt{3}} \\ \frac{2}{\sqrt{6}} & -\frac{1}{\sqrt{6}} & -\frac{1}{\sqrt{6}} \\ 0 & -\frac{1}{\sqrt{2}} & \frac{1}{\sqrt{2}} \end{pmatrix}. \quad (25)$$

Then, the mixing matrix V_q in the original base of S is transformed to $V_S V_q$ because the quark mass matrix is transformed as $V_S M_q^\dagger M_q V_S^\dagger$.

In conclusion, our quark mass matrices with the A_4 modular symmetry reproduce the observed CKM mixing matrix very well at nearby $\tau = i$. This successful result encourages us to investigate the lepton flavors in the same framework. We discuss the lepton sector with the A_4 modular symmetry in Sect. 5.

5 Lepton mass matrix in the A_4 modular invariance

5.1 Lepton mass matrix

The modular A_4 invariance also gives the lepton mass matrix in terms of the modulus τ which is common to both quarks and leptons if flavors of quarks and leptons are originated from a same two-dimensional compact space. We assign the A_4 representation and weight for leptons in Table 4, where the left-handed lepton doublets compose a A_4 triplet and the right-handed charged leptons are A_4 singlets. The weights of the leptons are assigned like the down-type quarks in Table 1.

Then, the superpotential of the charged lepton mass term is given in terms of modular forms of weight 2, $\mathbf{Y_3^{(2)}}$ since

Table 4 Assignments of representations and weights $-k_I$ for MSSM fields and modular forms of weight 2 and 4

	L	(e^c, μ^c, τ^c)	H_u	H_d	$\mathbf{Y_r^{(2)}}$, $\mathbf{Y_r^{(4)}}$
$SU(2)$	**2**	**1**	**2**	**2**	**1**
A_4	**3**	$(\mathbf{1}, \mathbf{1''}, \mathbf{1'})$	**1**	**1**	$\mathbf{3}$, $\{\mathbf{3}, \mathbf{1}, \mathbf{1'}\}$
$-k_I$	-2	(0, 0, 0)	0	0	2, 4

weights of the left-handed leptons and the right-handed charged leptons are -2 and 0, respectively. It is given as:

$$w_E = \alpha_e e^c H_d \mathbf{Y_3^{(2)}} L + \beta_e \mu^c H_d \mathbf{Y_3^{(2)}} L + \gamma_e \tau^c H_d \mathbf{Y_3^{(2)}} L, \tag{26}$$

where L is the left-handed A_4 triplet leptons. Taking (e_L, μ_L, τ_L) in the flavor base

the charged lepton mass matrix M_E is simply written as:

$$M_E = v_d \begin{pmatrix} \alpha_e & 0 & 0 \\ 0 & \beta_e & 0 \\ 0 & 0 & \gamma_e \end{pmatrix} \begin{pmatrix} Y_1 & Y_3 & Y_2 \\ Y_2 & Y_1 & Y_3 \\ Y_3 & Y_2 & Y_1 \end{pmatrix}_{RL}, \tag{27}$$

where coefficients α_e, β_e and γ_e are real parameters.

Suppose neutrinos to be Majorana particles. By using the Weinberg operator, the superpotential of the neutrino mass term, w_ν is given as:

$$w_\nu = -\frac{1}{\Lambda}(H_u H_u L L \mathbf{Y_r^{(4)}})_{\mathbf{1}}, \tag{28}$$

where Λ is a relevant cutoff scale. Since the left-handed lepton doublet has weight -2, the superpotential is given in terms of modular forms of weight 4, $\mathbf{Y_3^{(4)}}$, $\mathbf{Y_1^{(4)}}$ and $\mathbf{Y_{1'}^{(4)}}$.

By using the tensor products of A_4, we have

$$\begin{aligned} w_\nu = \frac{v_u^2}{\Lambda} \Bigg[& \begin{pmatrix} 2\nu_e\nu_e - \nu_\mu\nu_\tau - \nu_\tau\nu_\mu \\ 2\nu_\tau\nu_\tau - \nu_e\nu_\mu - \nu_\mu\nu_\tau \\ 2\nu_\mu\nu_\mu - \nu_\tau\nu_e - \nu_e\nu_\tau \end{pmatrix} \otimes \mathbf{Y_3^{(4)}} \\ & + (\nu_e\nu_e + \nu_\mu\nu_\tau + \nu_\tau\nu_\mu) \otimes g_{\nu 1} \mathbf{Y_1^{(4)}} \\ & (\nu_e\nu_\tau + \nu_\mu\nu_\mu + \nu_\tau\nu_e) \otimes g_{\nu 2} \mathbf{Y_{1'}^{(4)}} \Bigg] \\ = \frac{v_u^2}{\Lambda} [& (2\nu_e\nu_e - \nu_\mu\nu_\tau - \nu_\tau\nu_\mu) Y_1^{(4)} \\ & + (2\nu_\tau\nu_\tau - \nu_e\nu_\mu - \nu_\mu\nu_e) Y_3^{(4)} \\ & + (2\nu_\mu\nu_\mu - \nu_\tau\nu_e - \nu_e\nu_\tau) Y_2^{(4)} \\ & + (\nu_e\nu_e + \nu_\mu\nu_\tau + \nu_\tau\nu_\mu) g_{\nu 1} \mathbf{Y_1^{(4)}} \\ & + (\nu_e\nu_\tau + \nu_\mu\nu_\mu + \nu_\tau\nu_e) g_{\nu 2} \mathbf{Y_{1'}^{(4)}}], \end{aligned} \tag{29}$$

where $\mathbf{Y_3^{(4)}}$, $\mathbf{Y_1^{(4)}}$ and $\mathbf{Y_{1'}^{(4)}}$ are given in Eq. (13), and $g_{\nu 1}$, $g_{\nu 2}$ are complex parameters. The neutrino mass matrix is written as follows:

$$\begin{aligned} M_\nu = \frac{v_u^2}{\Lambda} \Bigg[& \begin{pmatrix} 2Y_1^{(4)} & -Y_3^{(4)} & -Y_2^{(4)} \\ -Y_3^{(4)} & 2Y_2^{(4)} & -Y_1^{(4)} \\ -Y_2^{(4)} & -Y_1^{(4)} & 2Y_3^{(4)} \end{pmatrix} + g_{\nu 1} \mathbf{Y_1^{(4)}} \begin{pmatrix} 1 & 0 & 0 \\ 0 & 0 & 1 \\ 0 & 1 & 0 \end{pmatrix} \\ & + g_{\nu 2} \mathbf{Y_{1'}^{(4)}} \begin{pmatrix} 0 & 0 & 1 \\ 0 & 1 & 0 \\ 1 & 0 & 0 \end{pmatrix} \Bigg]_{LL}. \end{aligned} \tag{30}$$

Then, the model parameters are α_e, β_e, γ_e, $g_{\nu 1}$ and $g_{\nu 2}$. Parameters α_e, β_e and γ_e are adjusted by the observed charged lepton masses. Therefore, the lepton mixing angles, the Dirac phase and Majorana phases are given by $g_{\nu 1}$ and $g_{\nu 2}$ in addition to the value of τ. Since τ is restricted in the narrow range for the quark sector as seen in Fig. 3, we can give some predictions in the lepton sector. Practically, we scan τ in $|\mathrm{Re}[\tau]| \leq 0.5$ and $\mathrm{Im}[\tau] \leq 2$ like in the analysis of quark mass matrices.

5.2 Numerical results of leptons

We input charged lepton masses in order to constrain the model parameters. We take Yukawa couplings of charged leptons at the GUT scale 2×10^{16} GeV, where $\tan\beta = 5$ is taken as well as quark Yukawa couplings [59,60]:

$$\begin{aligned} y_e &= (1.97 \pm 0.024) \times 10^{-6}, \\ y_\mu &= (4.16 \pm 0.050) \times 10^{-4}, \\ y_\tau &= (7.07 \pm 0.073) \times 10^{-3}, \end{aligned} \tag{31}$$

where lepton masses are given by $m_\ell = y_\ell v_H$ with $v_H = 174$ GeV. We also input the lepton mixing angles and neutrino mass parameters which are given by NuFit 4.1 in Table 5 [62]. We investigate two possible cases of neutrino masses m_i, which are the normal hierarchy (NH), $m_3 > m_2 > m_1$, and the inverted hierarchy (IH), $m_2 > m_1 > m_3$. Neutrino masses and the Pontecorvo–Maki–Nakagawa–Sakata (PMNS) matrix U_{PMNS} [63–65] are obtained by diagonalizing $M_E^\dagger M_E$ and $M_\nu^* M_\nu$. We also investigate the effective mass for the $0\nu\beta\beta$ decay, $\langle m_{ee} \rangle$ (see Appendix B) and the sum of three neutrino masses $\sum m_i$ since it is constrained by the recent cosmological data, which is the upper-bound $\sum m_i \leq 120$ meV obtained at the 95% confidence level [66–68].

Let us discuss numerical results for NH of neutrino masses. Since α_e/γ_e and β_e/γ_e are obtained by the observed charged lepton masses when τ is fixed, we input charged lepton masses to reduce free parameters. Parameters $g_{\nu 1}$ and $g_{\nu 2}$ are constrained by four observed quantities; three mixing angles of leptons and observed mass ratio $\Delta m^2_{\mathrm{sol}}/\Delta m^2_{\mathrm{atm}}$. In practice, the scanned ranges of $\mathrm{Im}[\tau]$ and $\mathrm{Re}[\tau]$ are $[\sqrt{3}/2, 2]$ and $[-1/2, 1/2]$, respectively, like for the quark sector. Neutrino couplings $|g_{\nu i}|$ are scanned in $[0,\ 10]$ while these phases are in $[-\pi, \pi]$. Indeed, we have obtained $|g_{\nu 1}| = 0.03$–1.15 and $|g_{\nu 1}| = 0.63$–1.22 in our numerical calculations.

At first, we show the allowed region on the $\mathrm{Re}[\tau]$–$\mathrm{Im}[\tau]$ plane in Fig. 4. Observed three mixing angles of leptons are reproduced at cyan, blue and red points. The sum of neutrino masses is consistent with the cosmological bound 120 meV at cyan points, but not at blue points. At red points, both CKM and PMNS are reproduced with the sum of neutrino masses

Table 5 The 3σ ranges of neutrino parameters from NuFIT 4.1 for NH and IH [62]

Observable	3σ range for NH	3σ range for IH
$\Delta m^2_{\rm atm}$	$(2.436\text{–}2.618) \times 10^{-3}\text{eV}^2$	$-(2.419\text{–}2.601) \times 10^{-3}\text{eV}^2$
$\Delta m^2_{\rm sol}$	$(6.79\text{–}8.01) \times 10^{-5}\text{eV}^2$	$(6.79\text{–}8.01) \times 10^{-5}\text{eV}^2$
$\sin^2\theta_{23}$	0.433–0.609	0.436–0.610
$\sin^2\theta_{12}$	0.275–0.350	0.275–0.350
$\sin^2\theta_{13}$	0.02044–0.02435	0.02064–0.02457

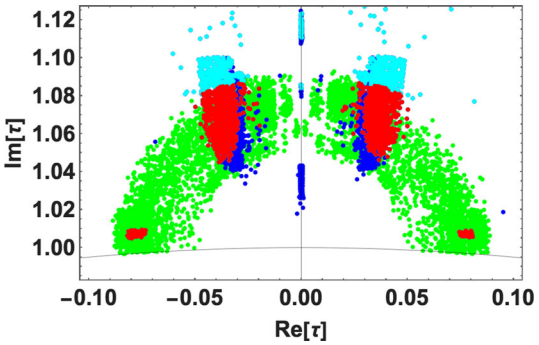

Fig. 4 Allowed regions of τ. PMNS mixing angles are reproduced at cyan, blue and red points while CKM are reproduced at green points. At cyan (blue) points, the sum of neutrino masses is below (above) 120 meV. At red points, both CKM and PMNS are reproduced with the sum of neutrino masses below 120 meV. The solid curve is the boundary of the fundamental domain, $|\tau| = 1$

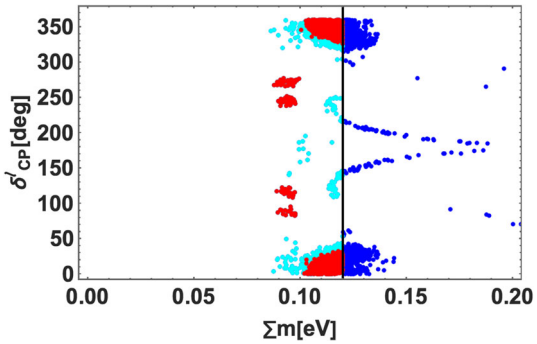

Fig. 6 Allowed region on the $\sum m_i$–δ^ℓ_{CP} plane, where the vertical solid line is the cosmological bound, for NH . Colors of points correspond to points of τ in Fig. 4

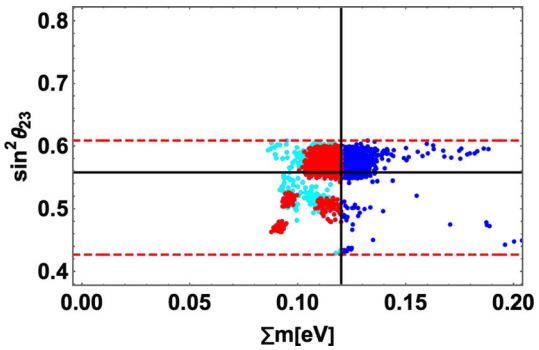

Fig. 5 Allowed region on $\sum m_i$–$\sin^2\theta_{23}$ plane, where the horizontal solid line denotes observed best-fit one, red dashed-lines denote the bound of 3σ interval, and the vertical line is the cosmological bound, for NH. Colors of points correspond to τ in Fig. 4

below 120 meV. For comparison, we add green points for quark CKM of Fig. 3. Allowed points of leptons are almost in $\text{Im}[\tau] \leq 1.12$ and $|\text{Re}[\tau]| \leq 0.1$.

The common τ causes the feedback in the quark sector. However, the tendency of $|V_{ub}|$, $|V_{cb}|$ and δ_{CP} are not so changed compared with Figs. 1 and 2 in the common region of τ.

We show the allowed region on the $\sum m_i$–$\sin^2\theta_{23}$ plane in Fig. 5, where colors (cyan, blue and red) of points correspond to points of τ in Fig. 4. Our prediction of the sum of neutrino masses is constrained by the cosmological bound as seen in Fig. 5. The minimal cosmological model, $\Lambda\text{CDM} + \sum m_i$, provides the upper-bound $\sum m_i <$ 120 meV [66,68] although it becomes weaker when the data are analysed in the context of extended cosmological models [61].

The red region, that is the common τ region for quarks and leptons, is constrained by the cosmological bound $\sum m_i =$ 120 meV. Then, the predicted sum of neutrino masses is 87–120 meV.

The cyan region is inconsistent with τ of quarks while the blue one is excluded by the cosmological bound $\sum m_i =$ 120 meV, although both are consistent with the data of NuFIT 4.1 [62]. The calculated $\sin^2\theta_{23}$ of the red region is distributed in restricted ranges. Therefore, the precise measurement of $\sin^2\theta_{23}$ and improving the bound of the sum of neutrino masses provide crucial tests for our scheme.

We show the allowed region on the $\sum m_i$–δ^ℓ_{CP} plane in Fig. 6. In the region of red points, δ^ℓ_{CP} is predicted to be in the restricted ranges, 0°–50°, 80°–100°, 110°–130°, 230°–250°, 260°–280° and 310°–360°. If the cosmological bound for the sum of neutrino masses will be improved, for example, it is 100 meV, δ^ℓ_{CP} is predicted in the distict range.

In Fig. 7, we plot δ^ℓ_{CP} versus $\sin^2\theta_{23}$ in order to see their correlation. Since there is a significant correlation between them, the precise measurement of $\sin^2\theta_{23}$ gives the clear prediction of δ^ℓ_{CP}.

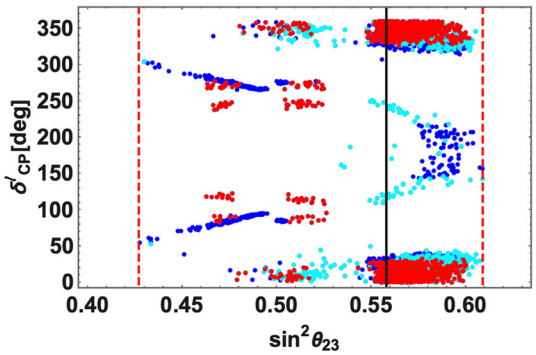

Fig. 7 Predicted δ^{ℓ}_{CP} versus $\sin^2\theta_{23}$, where the black line denotes observed best-fit value of $\sin^2\theta_{23}$, and red dashed-lines denote its upper(lower)-bound of 3σ interval for NH. Colors of points correspond to points of τ in Fig. 4

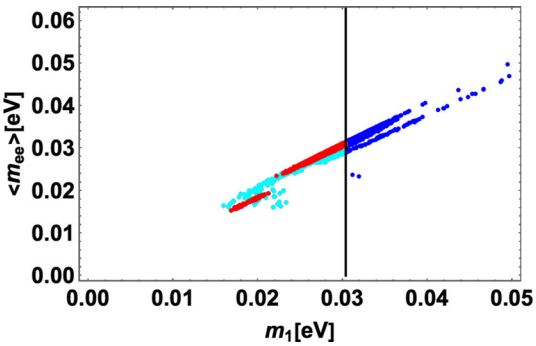

Fig. 8 Predicted effective mass $\langle m_{ee}\rangle$ of the $0\nu\beta\beta$ decay versus m_1 for NH. The vertical line is the upper-bound of m_1, which is derived from the cosmological bound, 120 meV. Colors of points correspond to points of τ in Fig. 4

Table 6 Numerical values of parameters and output of PMNS parameters at the best-fit point

τ	$-0.038+1.05\,i$
$g_{\nu 1}$	$0.061+0.274\,i$
$g_{\nu 2}$	$0.671-0.956\,i$
α_e/γ_e	6.71×10^{-2}
β_e/γ_e	1.24×10^{-3}
$\sin^2\theta_{12}$	0.305
$\sin^2\theta_{23}$	0.565
$\sin^2\theta_{13}$	0.0216
δ^{ℓ}_{CP}	27.4°
$\sum m_i$	118 meV
$\langle m_{ee}\rangle$	30.1 meV
χ^2	0.64

We can also predict the effective mass $\langle m_{ee}\rangle$ for the $0\nu\beta\beta$ decay versus the lightest mass m_1 as seen in Fig. 8. At the red point region, we predict $\langle m_{ee}\rangle = 15$–$31$ meV.

The predicted $\langle m_{ee}\rangle$ larger than 31 meV is excluded by the sum of neutrino masses.

In Table 6, we present best-fit values of parameters and outputs, where we input the common value $\tau = -0.038 + 1.05\,i$ in Table 3. In our χ^2 fit, δ^{ℓ}_{CP} is not included, but it is only an output because T2K and NOνA experiments have presented the best-fit values of δ^{ℓ}_{CP} with opposite sign each other [44,45]. Our predicted $\delta^{\ell}_{CP} = 27.4°$ in Table 6 is rather small. The systematic χ^2 fit of both quarks and leptons will be needed by including precise data of δ^{ℓ}_{CP} since $\delta^{\ell}_{CP} \simeq \pm 90°$ is also predicted in Fig. 6.

We also present the mixing matrices of charged leptons and neutrinos for the best-fit sample of Table 6. Those are given as:

$$U_\ell \approx \begin{pmatrix} 0.989 & 0.106-0.073\,i & 0.062-0.043\,i \\ -0.087-0.060\,i & 0.960 & -0.261+0.003\,i \\ -0.087-0.060\,i & 0.250+0.003\,i & 0.962 \end{pmatrix},$$
$$U_\nu \approx \begin{pmatrix} 0.732 & 0.465-0.459\,i & 0.097-0.166\,i \\ -0.333-0.267\,i & 0.228-0.115\,i & 0.868 \\ -0.415-0.332\,i & 0.713 & -0.448-0.094\,i \end{pmatrix}, \quad (32)$$

where $U_{\rm PMNS} = U_\ell^\dagger U_\nu$. They are also given in the diagonal base of the generator S in order to see the hierarchical structure of mixing like in the quark mixing matrix in Eq. (24), by using the unitary transformation of Eq. (25). It is noticed that the mixing matrix of charged leptons U_ℓ is similar to the quark mixing matrices of Eq. (24). On the other hand, two large mixing angles appear in the neutrino mixing matrix U_ν.

In our numerical calculations, we have not included the RGE effects in the lepton mixing angles and neutrino mass ratio $\Delta m^2_{\rm sol}/\Delta m^2_{\rm atm}$. We suppose that those corrections are very small between the electroweak and GUT scales for NH of neutrino masses. This assumption is justified well in the case of $\tan\beta \leq 5$ unless neutrino masses are almost degenerate [26].

Finally, we discuss briefly the case of IH of neutrino masses. Indeed, there is a very small region of the common τ for quarks and leptons, which is marginal since the sum of neutrino masses is very close to the cosmological bound, 120 meV. Therefore, we omit discussions of this case.

6 Summary

We have studied both quark and lepton mass matrices in the A_4 modular symmetry towards the unification of quark and lepton flavors. If flavors of quarks and leptons are originated from a same two-dimensional compact space, quarks and leptons have the same flavor symmetry and the same value of the modulus τ.

For the quark sector, we have adopted modular forms of weights 2 and 6. We have presented the viable model for quark mass matrices, in which the down-type quark mass matrix is constructed by modular forms of weight 2 while the up-type quark mass matrix is constructed by modular

forms of weight 6. In the lepton sector, the charged lepton mass matrix is constructed by modular forms of weight 2 while modular forms of weight 4 is used for the neutrino mass matrix, which is generated by the Weinberg operator.

The viable region close to $\tau = i$ is obtained in our quark mass matrices.

Lepton mass matrices also work well at nearby $\tau = i$, which overlaps with the one of the quark sector, for NH of neutrino masses. In the common τ region for quarks and leptons, the predicted sum of neutrino masses is 87–120 meV taking account of its cosmological bound. Since both the Dirac CP phase δ^{ℓ}_{CP} and $\sin^2\theta_{23}$ are correlated significantly with the sum of neutrino masses, improving its cosmological bound provides crucial tests for our scheme as well as the precise measurement of $\sin^2\theta_{23}$ and δ^{ℓ}_{CP}. The effective neutrino mass of the $0\nu\beta\beta$ decay is predicted to be $\langle m_{ee}\rangle = 15$–$31$ meV. The IH of neutrino masses is almost excluded by the cosmological bound of the sum of neutrino masses.

It is remarked that the common τ is fixed at nearby $\tau = i$ in the fundamental domain of SL(2, Z), which suggests the residual symmetry Z_2 in the quark and lepton mass matrices. Some corrections could violate the exact symmetry. It is also emphasized that the spontaneous CP violation in Type IIB string theory is possibly realized at nearby $\tau = i$, where the moduli stabilization as well as the calculation of Yukawa couplings is performed in a controlled way [69]. Thus, our phenomenological result of the modulus τ is favored in the theoretical investigation.

Acknowledgements This research was supported by an appointment to the JRG Program at the APCTP through the Science and Technology Promotion Fund and Lottery Fund of the Korean Government. This was also supported by the Korean Local Governments—Gyeongsangbuk-do Province and Pohang City (H. O.). H. O. is sincerely grateful for the KIAS member.

Data Availability Statement This manuscript has no associated data or the data will not be deposited. [Authors' comment: This issue is based on ref. [69].]

Funded by SCOAP[3].

Appendix

Appendix A: Tensor product of A_4 group

We take the generators of A_4 group for the triplet as follows:

$$S = \frac{1}{3}\begin{pmatrix} -1 & 2 & 2 \\ 2 & -1 & 2 \\ 2 & 2 & -1 \end{pmatrix}, \qquad T = \begin{pmatrix} 1 & 0 & 0 \\ 0 & \omega & 0 \\ 0 & 0 & \omega^2 \end{pmatrix}, \tag{33}$$

where $\omega = e^{i\frac{2}{3}\pi}$ for a triplet. In this base, the multiplication rule is

$$\begin{aligned} &\begin{pmatrix} a_1 \\ a_2 \\ a_3 \end{pmatrix}_{\mathbf{3}} \otimes \begin{pmatrix} b_1 \\ b_2 \\ b_3 \end{pmatrix}_{\mathbf{3}} \\ &= (a_1b_1 + a_2b_3 + a_3b_2)_{\mathbf{1}} \oplus (a_3b_3 + a_1b_2 + a_2b_1)_{\mathbf{1}'} \\ &\quad \oplus (a_2b_2 + a_1b_3 + a_3b_1)_{\mathbf{1}''} \\ &\quad \oplus \frac{1}{3}\begin{pmatrix} 2a_1b_1 - a_2b_3 - a_3b_2 \\ 2a_3b_3 - a_1b_2 - a_2b_1 \\ 2a_2b_2 - a_1b_3 - a_3b_1 \end{pmatrix}_{\mathbf{3}} \\ &\quad \oplus \frac{1}{2}\begin{pmatrix} a_2b_3 - a_3b_2 \\ a_1b_2 - a_2b_1 \\ a_3b_1 - a_1b_3 \end{pmatrix}_{\mathbf{3}}, \end{aligned}$$

$$\begin{aligned} &\mathbf{1} \otimes \mathbf{1} = \mathbf{1}, \qquad \mathbf{1}' \otimes \mathbf{1}' = \mathbf{1}'', \qquad \mathbf{1}'' \otimes \mathbf{1}'' = \mathbf{1}', \\ &\mathbf{1}' \otimes \mathbf{1}'' = \mathbf{1}, \end{aligned} \tag{34}$$

where

$$T(\mathbf{1}') = \omega, \qquad T(\mathbf{1}'') = \omega^2. \tag{35}$$

More details are shown in the review [6,7].

Appendix B: Majorana and Dirac phases and $\langle m_{ee}\rangle$ in $0\nu\beta\beta$ decay

Supposing neutrinos to be Majorana particles, the PMNS matrix $U_{\rm PMNS}$ [63,64] is parametrized in terms of the three mixing angles θ_{ij} $(i, j = 1, 2, 3;\ i < j)$, one CP violating Dirac phase $\delta_{\rm CP}$ and two Majorana phases α_{21}, α_{31} as follows:

$$\begin{aligned} U_{\rm PMNS} &= \begin{pmatrix} c_{12}c_{13} & s_{12}c_{13} & s_{13}e^{-i\delta^{\ell}_{\rm CP}} \\ -s_{12}c_{23} - c_{12}s_{23}s_{13}e^{i\delta^{\ell}_{\rm CP}} & c_{12}c_{23} - s_{12}s_{23}s_{13}e^{i\delta^{\ell}_{\rm CP}} & s_{23}c_{13} \\ s_{12}s_{23} - c_{12}c_{23}s_{13}e^{i\delta^{\ell}_{\rm CP}} & -c_{12}s_{23} - s_{12}c_{23}s_{13}e^{i\delta^{\ell}_{\rm CP}} & c_{23}c_{13} \end{pmatrix} \\ &\times \begin{pmatrix} 1 & 0 & 0 \\ 0 & e^{i\frac{\alpha_{21}}{2}} & 0 \\ 0 & 0 & e^{i\frac{\alpha_{31}}{2}} \end{pmatrix}, \end{aligned} \tag{36}$$

where c_{ij} and s_{ij} denote $\cos\theta_{ij}$ and $\sin\theta_{ij}$, respectively.

The rephasing invariant CP violating measure of leptons [70,71] is defined by the PMNS matrix elements $U_{\alpha i}$. It is written in terms of the mixing angles and the CP violating phase as:

$$J_{CP} = \mathrm{Im}\left[U_{e1}U_{\mu 2}U_{e2}^{*}U_{\mu 1}^{*}\right] = s_{23}c_{23}s_{12}c_{12}s_{13}c_{13}^{2}\sin\delta_{\mathrm{CP}}^{\ell}, \tag{37}$$

where $U_{\alpha i}$ denotes the each component of the PMNS matrix.

There are also other invariants I_1 and I_2 associated with Majorana phases

$$\begin{aligned} I_1 &= \mathrm{Im}\left[U_{e1}^{*}U_{e2}\right] = c_{12}s_{12}c_{13}^{2}\sin\left(\frac{\alpha_{21}}{2}\right), \\ I_2 &= \mathrm{Im}\left[U_{e1}^{*}U_{e3}\right] = c_{12}s_{13}c_{13}\sin\left(\frac{\alpha_{31}}{2} - \delta_{\mathrm{CP}}^{\ell}\right). \end{aligned} \tag{38}$$

We can calculate $\delta_{\mathrm{CP}}^{\ell}$, α_{21} and α_{31} with these relations by taking account of

$$\begin{aligned} \cos\delta_{CP}^{\ell} &= \frac{|U_{\tau 1}|^2 - s_{12}^2 s_{23}^2 - c_{12}^2 c_{23}^2 s_{13}^2}{2c_{12}s_{12}c_{23}s_{23}s_{13}}, \\ \mathrm{Re}\left[U_{e1}^{*}U_{e2}\right] &= c_{12}s_{12}c_{13}^{2}\cos\left(\frac{\alpha_{21}}{2}\right), \\ \mathrm{Re}\left[U_{e1}^{*}U_{e3}\right] &= c_{12}s_{13}c_{13}\cos\left(\frac{\alpha_{31}}{2} - \delta_{\mathrm{CP}}^{\ell}\right). \end{aligned} \tag{39}$$

In terms of this parametrization, the effective mass for the $0\nu\beta\beta$ decay is given as follows:

$$\langle m_{ee}\rangle = |m_1 c_{12}^2 c_{13}^2 + m_2 s_{12}^2 c_{13}^2 e^{i\alpha_{21}} + m_3 s_{13}^2 e^{i(\alpha_{31} - 2\delta_{CP}^{\ell})}|. \tag{40}$$

References

1. S. Pakvasa, H. Sugawara, Phys. Lett. **73B**, 61 (1978)
2. F. Wilczek, A. Zee, Phys. Lett. **70B** (1977) [418 Erratum: Phys. Lett. **72B** (1978) 504]
3. M. Fukugita, M. Tanimoto, T. Yanagida, Phys. Rev. D **57**, 4429 (1998). arXiv:hep-ph/9709388
4. Y. Fukuda et al., Super-Kamiokande Collaboration, Phys. Rev. Lett. **81**, 1562 (1998). arXiv:hep-ex/9807003
5. G. Altarelli, F. Feruglio, Rev. Mod. Phys. **82**, 2701 (2010). arXiv:1002.0211 [hep-ph]
6. H. Ishimori, T. Kobayashi, H. Ohki, Y. Shimizu, H. Okada, M. Tanimoto, Prog. Theor. Phys. Suppl. **183**, 1 (2010). arXiv:1003.3552 [hep-th]
7. H. Ishimori, T. Kobayashi, H. Ohki, H. Okada, Y. Shimizu, M. Tanimoto, Lect. Notes Phys. **858**, 1 (2012)
8. D. Hernandez, A.Y. Smirnov, Phys. Rev. D **86**, 053014 (2012). arXiv:1204.0445 [hep-ph]
9. S.F. King, C. Luhn, Rep. Prog. Phys. **76**, 056201 (2013). arXiv:1301.1340 [hep-ph]
10. S.F. King, A. Merle, S. Morisi, Y. Shimizu, M. Tanimoto, New J. Phys. **16**, 045018 (2014). arXiv:1402.4271 [hep-ph]
11. M. Tanimoto, AIP Conf. Proc. **1666**, 120002 (2015)
12. S.F. King, Prog. Part. Nucl. Phys. **94**, 217 (2017). arXiv:1701.04413 [hep-ph]
13. S.T. Petcov, Eur. Phys. J. C **78**(9), 709 (2018). arXiv:1711.10806 [hep-ph]
14. E. Ma, G. Rajasekaran, Phys. Rev. D **64**, 113012 (2001). arXiv:hep-ph/0106291
15. K.S. Babu, E. Ma, J.W.F. Valle, Phys. Lett. B **552**, 207 (2003). arXiv:hep-ph/0206292
16. G. Altarelli, F. Feruglio, Nucl. Phys. B **720**, 64 (2005). arXiv:hep-ph/0504165
17. G. Altarelli, F. Feruglio, Nucl. Phys. B **741**, 215 (2006). arXiv:hep-ph/0512103
18. Y. Shimizu, M. Tanimoto, A. Watanabe, Prog. Theor. Phys. **126**, 81 (2011). arXiv:1105.2929 [hep-ph]
19. S.T. Petcov, A.V. Titov, Phys. Rev. D **97**(11), 115045 (2018). arXiv:1804.00182 [hep-ph]
20. S.K. Kang, Y. Shimizu, K. Takagi, S. Takahashi, M. Tanimoto, PTEP **2018**(8), 083B01 (2018). arXiv:1804.10468 [hep-ph]
21. F. Feruglio, in *From My Vast Repertoire ...: Guido Altarelli's Legacy*, A. Levy, S. Forte, Stefano, and G. Ridolfi, eds., pp.227–266 (2019). arXiv:1706.08749 [hep-ph]
22. R. de Adelhart Toorop, F. Feruglio, C. Hagedorn, Nucl. Phys. B **858**, 437 (2012). arXiv:1112.1340 [hep-ph]
23. T. Kobayashi, K. Tanaka, T.H. Tatsuishi, Phys. Rev. D **98**(1), 016004 (2018). arXiv:1803.10391 [hep-ph]
24. J.T. Penedo, S.T. Petcov, Nucl. Phys. B **939**, 292 (2019). arXiv:1806.11040 [hep-ph]
25. P.P. Novichkov, J.T. Penedo, S.T. Petcov, A.V. Titov, JHEP **1904**, 174 (2019). arXiv:1812.02158 [hep-ph]
26. J.C. Criado, F. Feruglio, Sci. Post Phys. **5**(5), 042 (2018). arXiv:1807.01125 [hep-ph]
27. T. Kobayashi, N. Omoto, Y. Shimizu, K. Takagi, M. Tanimoto, T.H. Tatsuishi, JHEP **1811**, 196 (2018). arXiv:1808.03012 [hep-ph]
28. P.P. Novichkov, J.T. Penedo, S.T. Petcov, A.V. Titov, JHEP **1904**, 005 (2019). arXiv:1811.04933 [hep-ph]
29. T. Kobayashi, Y. Shimizu, K. Takagi, M. Tanimoto, T.H. Tatsuishi, JHEP **02**, 097 (2020). arXiv:1907.09141 [hep-ph]
30. G.J. Ding, S.F. King, X.G. Liu, Phys. Rev. D **100**(11), 115005 (2019). arXiv:1903.12588 [hep-ph]
31. X.G. Liu, G.J. Ding, JHEP **1908**, 134 (2019). arXiv:1907.01488 [hep-ph]
32. F.J. de Anda, S.F. King, E. Perdomo, Phys. Rev. D **101**(1), 015028 (2020). arXiv:1812.05620 [hep-ph]
33. P.P. Novichkov, S.T. Petcov, M. Tanimoto, Phys. Lett. B **793**, 247 (2019). arXiv:1812.11289 [hep-ph]
34. T. Kobayashi, S. Tamba, Phys. Rev. D **99**(4), 046001 (2019). arXiv:1811.11384 [hep-th]
35. A. Baur, H.P. Nilles, A. Trautner, P.K.S. Vaudrevange, Phys. Lett. B **795**, 7 (2019). arXiv:1901.03251 [hep-th]
36. I. de Medeiros Varzielas, S.F. King, Y.L. Zhou, Phys. Rev. D **101**(5), 055033 (2020). arXiv:1906.02208 [hep-ph]
37. P.P. Novichkov, J.T. Penedo, S.T. Petcov, A.V. Titov, JHEP **1907**, 165 (2019). arXiv:1905.11970 [hep-ph]
38. T. Kobayashi, Y. Shimizu, K. Takagi, M. Tanimoto, T.H. Tatsuishi, H. Uchida, Phys. Lett. B **794**, 114 (2019). arXiv:1812.11072 [hep-ph]
39. T. Kobayashi, Y. Shimizu, K. Takagi, M. Tanimoto, T.H. Tatsuishi, PTEP **2020**(5), 053B05 (2020). arXiv:1906.10341 [hep-ph]
40. H. Okada, M. Tanimoto, Phys. Lett. B **791**, 54 (2019). arXiv:1812.09677 [hep-ph]
41. T. Nomura, H. Okada, Phys. Lett. B **797**, 134799 (2019). arXiv:1904.03937 [hep-ph]
42. H. Okada, Y. Orikasa, Phys. Rev. D **100**(11), 115037 (2019). arXiv:1907.04716 [hep-ph]
43. Y. Kariyazono, T. Kobayashi, S. Takada, S. Tamba, H. Uchida, Phys. Rev. D **100**(4), 045014 (2019). arXiv:1904.07546 [hep-th]
44. K. Abe et al., T2K Collaboration, Nature **580**, 339 (2020)
45. P. Adamson et al. [NOvA Collaboration], Phys. Rev. Lett. **118**(23), 231801 (2017). arXiv:1703.03328 [hep-ex]
46. H. Okada, M. Tanimoto, arXiv:2005.00775 [hep-ph]

47. J. Lauer, J. Mas, H.P. Nilles, Phys. Lett. B **226**, 251 (1989)
48. J. Lauer, J. Mas, H.P. Nilles, Nucl. Phys. B **351**, 353 (1991)
49. W. Lerche, D. Lust, N.P. Warner, Phys. Lett. B **231**, 417 (1989)
50. S. Ferrara, D. Lust, S. Theisen, Phys. Lett. B **233**, 147 (1989)
51. D. Cremades, L.E. Ibanez, F. Marchesano, JHEP **0405**, 079 (2004). arXiv:hep-th/0404229
52. T. Kobayashi, S. Nagamoto, Phys. Rev. D **96**(9), 096011 (2017). arXiv:1709.09784 [hep-th]
53. T. Kobayashi, S. Nagamoto, S. Takada, S. Tamba, T.H. Tatsuishi, Phys. Rev. D **97**(11), 116002 (2018). arXiv:1804.06644 [hep-th]
54. S. Ferrara, D. Lust, A.D. Shapere, S. Theisen, Phys. Lett. B **225**, 363 (1989)
55. M. Chen, S. Ramos-Sánchez, M. Ratz, Phys. Lett. B **801**, 135153 (2020). arXiv:1909.06910 [hep-ph]
56. R.C. Gunning, *Lectures on Modular Forms* (Princeton University Press, Princeton, 1962)
57. B. Schoeneberg, *Elliptic Modular Functions* (Springer, Berlin, 1974)
58. N. Koblitz, *Introduction to Elliptic Curves and Modular Forms* (Springer, Berlin, 1984)
59. S. Antusch, V. Maurer, JHEP **1311**, 115 (2013). arXiv:1306.6879 [hep-ph]
60. F. Björkeroth, F.J. de Anda, I. de Medeiros Varzielas, S.F. King, JHEP **1506**, 141 (2015)
61. M. Tanabashi et al. [Particle Data Group], Phys. Rev. D **98**(3), 030001 (2018)
62. I. Esteban, M.C. Gonzalez-Garcia, A. Hernandez-Cabezudo, M. Maltoni, T. Schwetz, JHEP **1901**, 106 (2019). arXiv:1811.05487 [hep-ph]
63. Z. Maki, M. Nakagawa, S. Sakata, Prog. Theor. Phys. **28**, 870 (1962)
64. B. Pontecorvo, Sov. Phys. JETP **26**, 984 (1968)
65. B. Pontecorvo, Zh Eksp, Teor. Fiz. **53**, 1717 (1967)
66. S. Vagnozzi, E. Giusarma, O. Mena, K. Freese, M. Gerbino, S. Ho, M. Lattanzi, Phys. Rev. D **96**(12), 123503 (2017). arXiv:1701.08172 [astro-ph.CO]
67. N. Aghanim et al. [Planck], arXiv:1807.06209 [astro-ph.CO]
68. N. Aghanim et al. [Planck Collaboration], arXiv:1807.06209 [astro-ph.CO]
69. T. Kobayashi, H. Otsuka, Phys. Rev. D **102**(2), 026004 (2020). arXiv:2004.04518 [hep-th]
70. C. Jarlskog, Phys. Rev. Lett. **55**, 1039 (1985)
71. P.I. Krastev, S.T. Petcov, Phys. Lett. B **205**, 84 (1988)